10-1-2019

Acoustic end corrections for micro-perforated plates

Vahid Naderyan
University of Mississippi

Richard Raspet
University of Mississippi

Craig J. Hickey
University of Mississippi

Mohammad Mohammadi
University of Mississippi

Recommended Citation

Naderyan, V., Raspet, R., Hickey, C. J., & Mohammadi, M. (2019). Acoustic end corrections for micro-perforated plates. The Journal of the Acoustical Society of America, 146(4), EL399–EL404. https://doi.org/10.1121/1.5129560

Acoustic end corrections for micro-perforated plates

Vahid Naderyan, Richard Raspet, Craig J. Hickey, and Mohammad Mohammadi

Citation: The Journal of the Acoustical Society of America **146**, EL399 (2019); doi: 10.1121/1.5129560
View online: https://doi.org/10.1121/1.5129560
View Table of Contents: https://asa.scitation.org/toc/jas/146/4
Published by the Acoustical Society of America

Acoustic end corrections for micro-perforated plates

Vahid Naderyan, Richard Raspet, and Craig J. Hickey
Department of Physics and Astronomy, National Center for Physical Acoustics, University of Mississippi, University, Mississippi 38677, USA
vahid.nad@gmail.com; raspet@olemiss.edu; chickey@olemiss.edu

Mohammad Mohammadi
National Center for Physical Acoustics, University of Mississippi, University, Mississippi 38677, USA
m.mohammadi@outlook.com

Abstract: Micro-perforated plates (MPPs) are acoustically important elements in micro-electro-mechanical systems (MEMS). In this work an analytical solution for perforated plates is combined with finite element method (FEM) to develop formulas for the reactive and resistive end effects of the perforations on the plate. The reactive end effect is found to depend on the hole radius and porosity. The resistive end effect is found to depend on hole radius only. FEM is also used to develop an understanding of the loss mechanism that corresponds to the resistive end effects. The developed models can be used in optimization studies of the MEMS and MPPs.

[CCC]
Date Received: July 20, 2019 **Date Accepted:** September 29, 2019

1. Introduction

Many micro-electro-mechanical systems (MEMS) devices include a fixed micro-perforated plate. In MEMS devices, such as microphones and accelerometers, the perforations are designed to minimize damping between the moving and the fixed plates. This damping phenomenon, often called squeezed-film damping, is typically one of the major sources of noise in MEMS sensors (Kuntzman *et al.*, 2018) and has been a subject of study in MEMS research (Younis, 2011). The squeezed-film damping includes the damping of the squeezed air between two plates as well as the damping of the air moving in and out through the perforations. The damping of the perforations includes losses inside the holes as well as the so-called "end effects." As air flows into and out of the perforations, the air adjacent to the ends of the holes will be disturbed on both sides of the plate, which is called the end effect.

Micro-perforated plates (MPPs) are widely used as sound absorption materials in many noise control applications (Maa, 1998). Therefore, several research studies have been conducted on the acoustic properties of the perforations over the past few decades, for the MPP applications. Maa (1998) developed a solution for MPP impedance based on a model of oscillatory, viscous flow in cylindrical tubes which included end corrections for both resistive and reactive parts of the impedance. Several models for the impedance of the MPPs have been proposed after Maa. Although most of the models are in agreement about the hole impedance, there is not a general consensus on the end corrections, especially the resistive end correction.

FEM can be used to study the acoustic behavior of MEMS devices. However, using FEM simulations for the calculations of the total response of the system is computationally expensive, time consuming, and inconvenient. Hence, analytical formulas are desirable to use in calculations for optimizing the MEMS. In the present work, we utilize the analytical solutions and FEM to derive formulas for the impedance of the perforated plate component of the MEMS. First, an analytical solution for the impedance of the perforated plates is derived using the low reduced-frequency (LRF) method. Then FEM is used to calculate the resistive and reactive end corrections for micro-perforated plates for a wide range of porosities applicable to both MEMS studies and MPP studies.

2. Impedance of micro-perforated plates

Here we use the LRF method for visco-thermal sound propagation in cylindrical pores developed by Tijdeman (1975) to solve for the specific acoustic impedance of the

micro-perforated plates. A schematic cross-section view of the perforated plate is shown in Fig. 1(a).

For a cylindrical hole with an acoustic plane wave incident from the bottom, if we assume the length (l) is large enough compared to the hole radius (so that the end effects are negligible) and assume continuous pressure and volume velocity boundary conditions at the interface, using the LRF method we find the intrinsic specific acoustic impedance to be

$$Z_s = \frac{1}{\phi\sqrt{f(\lambda)\left[\gamma-(\gamma-1)f(\lambda_T)\right]}}, \tag{1}$$

where $\lambda = r\sqrt{\rho_0\omega/\mu}$ is the dimensionless shear wave-number, $\lambda_T = r\sqrt{\rho_0 c_p\omega/\kappa}$ is the dimensionless thermal wave-number, r is the hole radius, ρ_0 is the air density, ω is the angular frequency, μ is the viscosity, c_p is the specific heat at constant pressure, κ is the thermal conductivity, ϕ is the porosity (ratio of the holes area to the total plate area including the holes area), and we have defined

$$f(\lambda) = 1 - \frac{2J_1\left(\sqrt{i}\lambda\right)}{\sqrt{i}\lambda J_0\left(\sqrt{i}\lambda\right)}, \tag{2}$$

where J_0 and J_1 are Bessel functions of the first kind of zeroth and first order, respectively. Then using the impedance-translation theorem (Pierce, 1981), the dimensionless specific acoustic impedance of the perforated plate is calculated

$$Z = Z_s\left[\frac{\cos(kl) - iZ_s\sin(kl)}{Z_s\cos(kl) - i\sin(kl)}\right] - 1, \tag{3}$$

where c_0 is the velocity of sound and

$$k = (\omega/c_0)\sqrt{(\gamma-(\gamma-1)f(\lambda_T))/f(\lambda)}. \tag{4}$$

This solution includes both viscous and thermal losses. End effects are not included in this solution. For plates with finite thickness, the end effects are significant and have to be incorporated into the solution.

Maa's solution which does not include the thermal losses is

$$Z = \frac{i\omega l}{\phi c_0}\left[\frac{\sqrt{i}\lambda J_0\left(\sqrt{i}\lambda\right)}{\sqrt{i}\lambda J_0\left(\sqrt{i}\lambda\right) - 2J_1\left(\sqrt{i}\lambda\right)}\right]. \tag{5}$$

It has been widely used by researchers for the impedance of perforated plates. For the range of the parameters used in the present study, the LRF solution, Eq. (3), is very close to Maa solution, Eq. (5). Equations (3) and (5) do not include the end effects. The main difference in the different MPP impedance solutions presented in the literature is the way that the end corrections have been treated.

2.1 Reactive end correction

When the mass of air oscillates within the hole it travels a distance further than the geometric thickness of the hole. The actual mass of the moving air is more than the mass of the air inside the hole. This effect has been taken into account by adding a correction length to the actual thickness of the hole (reactive end correction). Rayleigh (1877) calculated the reactive end correction to be $16r/3\pi$, including both sides of the

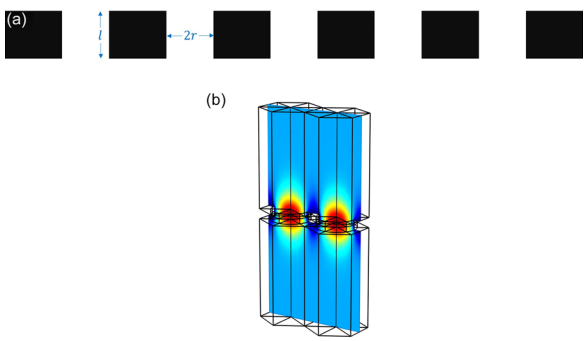

Fig. 1. (Color online) (a) Schematic cross-section view of a perforated plate. (b) Velocity at 1000 Hz in the 3 D FEM domain for two adjacent cells.

hole. Sivian (1935) proposed using Rayleigh's value for both reactive and resistive end corrections. However, he used two different values for the viscosity of the air inside the hole with thermally conducting surface and for the end correction region with a non-thermally conducting medium.

At high porosities when the spacing between the holes is small, the flows on sides of the plate can interfere with each other. This interaction effect leads to a reduction in the total reactive end effect. Fok (Melling, 1973), assuming an infinitely thin plate, developed a formula for the interaction effect

$$\Psi_{Fok}(\phi) = 1 - 1.409\sqrt{\phi} + 0.338\sqrt{\phi^3} + 0.068\sqrt{\phi^5} - 0.023\sqrt{\phi^6} + \cdots. \tag{6}$$

Melling (1973) multiplied the Rayleigh's formula by the Fok function to take into account the interaction effect.

Schultz *et al.* (2009) used Rayleigh's value multiplied by the Fok function for both reactance and resistance end corrections. Mechel and Munjal (2008) proposed another variant of the interaction function

$$\Psi_{Mechel}(\phi) = \begin{cases} 1 - 1.323\sqrt{\phi} & 0 < \phi < 0.23, \\ 0.786 - 0.825\sqrt{\phi} & 0.23 < \phi < 0.91. \end{cases} \tag{7}$$

In this work, we use Thermoviscous Acoustics module of the COMSOL FEM simulation software to calculate the end effects for a hexagonal pattern of holes in the frequency domain. Due to the uniform repetitive pattern of the holes only a single cell (a hole and the hexagonal area surrounding it) is modeled. Also, due to the hexagonal symmetry of the cell, a 3 D model that includes one-sixth of a cell is modeled. Symmetry boundary condition is applied to the side edges of the cell to represent an infinite periodic arrangement of holes. On the bottom side of the plate, an inlet velocity is applied to a surface far enough from the plate to ensure a uniform plane wave incidence to the plate. On the top side of the plate and far from the plate a perfectly matched layer (PML) is placed which mimics infinite open air with no reflections. Isothermal and no-slip boundary conditions are applied to all surfaces of the plate. Finite elements with quadratic velocity and temperature shape functions, and linear pressure shape functions are used (Kampinga, 2010). Figure 1(b) shows a cross-section of the velocity at 1000 Hz in the FEM domain for two adjacent cells where the plate thickness is 3 μm, porosity is 0.5, the air layer thickness on each side is 30 μm, and the thickness of the PML is 10 μm.

The specific acoustic impedance from the FEM is calculated from

$$Z_{FEM} = \frac{P_t - P_b}{\rho_0 c_0 Q}, \tag{8}$$

where $P_t - P_b$ is the pressure difference between the top and bottom of the hole, and Q is the mean velocity in the hole. Then an additional thickness (l_{ei}) is added to the actual thickness of the plate (l) in Eq. (3) to take into account for the end effects. The reactive end length correction (l_{ei}) is determined by varying it to fit the imaginary part of the theoretical impedance [Eq. (3)] to the impedance calculated from the FEM.

A set of numerical simulations were conducted for porosities from 0.01 to 0.7, the pitch values from 8 to 24 μm, and for plate thicknesses from 1 to 3 μm. Pitch is defined as the center-to-center distance between adjacent holes. The reactive end length correction was found to be a function of hole radius and porosity. The data were found to fit the form

$$l_{ei} = \frac{16r}{3\pi}\left(1 - \sqrt{\phi}\right) \tag{9}$$

using a least square method ($R^2 = 0.98$). At very low porosities, where the interaction effects are negligible, this solution converges to Rayleigh's solution. The interaction effect was found to be a simple function of the porosity

$$\Psi(\phi) = 1 - \sqrt{\phi}. \tag{10}$$

In Fig. 2 the proposed interaction function, Eq. (10), is compared with Fok's function and Mechel's function.

As shown in the figure, the correction function tends to unity as the porosity tends to zero. At larger porosities as the holes get closer to each other the interaction effects on both sides of the plates reduce the total end effect, so the interaction function decreases as porosities increases. The proposed simple function predicts smaller correction values compared to the other two models.

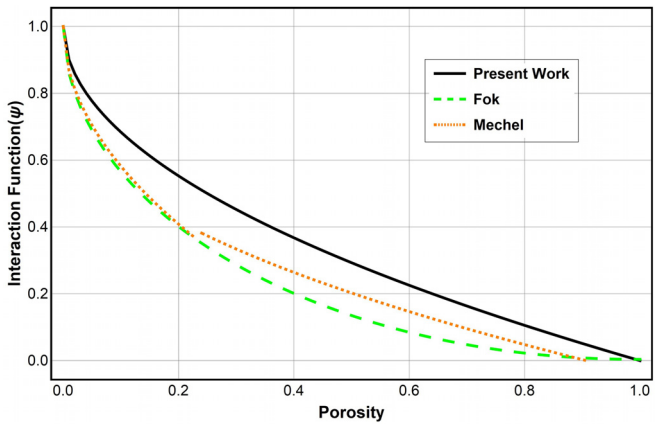

Fig. 2. (Color online) Comparison of the interaction functions.

In Fig. 3 the reactive part of the normalized impedance calculated using the Rayleigh's end correction without any interaction correction, using the Fok function for the interaction corrections, and also using the proposed model [Eq. (9)] are compared with the results of COMSOL FEM simulations for a perforated plate with 3 μm thickness and 16 μm pitch at 1000 Hz. As can be seen, all models are in a good agreement at low porosities. They deviate from each other as the porosity increases. The result given by the proposed formula is in a good agreement with the numerical results in the whole range of porosities.

2.2 Resistive end correction

In previous studies, the source of the resistive end effect has been hypothesized to be due to the surface energy dissipation due to the friction of the air at the surface of the plate on both sides of the hole, as air moves in and out of the hole. This end effect adds additional resistance to the resistance inside the holes. Prediction of this dissipation effect is not trivial. Sivian (1935) used Rayleigh's length correction value (proposed for the reactive part) for both reactive and resistive end corrections. Ingard (1953) defined $R_s = 0.5\sqrt{2\mu\rho_0\omega}$ as the surface resistance, and calculated a resistance correction of $R_e = 2R_s$ to be added to the hole resistance. However, his experimental results suggest using $4R_s$ instead. Melling (1973) and Schultz *et al.* (2009) used the same end correction used for the reactive part (Rayleigh's value multiplied by the Fok function) for the resistive end length correction also. Guo *et al.* (2008) suggested using $2\alpha R_s$ where $\alpha = 2$ for holes with round edges and $\alpha = 4$ for holes with sharp edges. Bolton and Kim (2010) used a time-domain incompressible computational fluid dynamics model to numerically calculate α. They showed that α exhibits a dependence on frequency, plate thickness, hole radius, and porosity. However, the dependence on porosity was negligible and using curve fitting to the numerical results α was defined as

$$\alpha = (14.1(l/2r) + 117)\sqrt{\mathrm{f}}, \tag{11}$$

where f is the frequency. Temiz *et al.* (2014) used a similar approach for an incompressible fluid in the frequency domain to calculate a formula for the end corrections

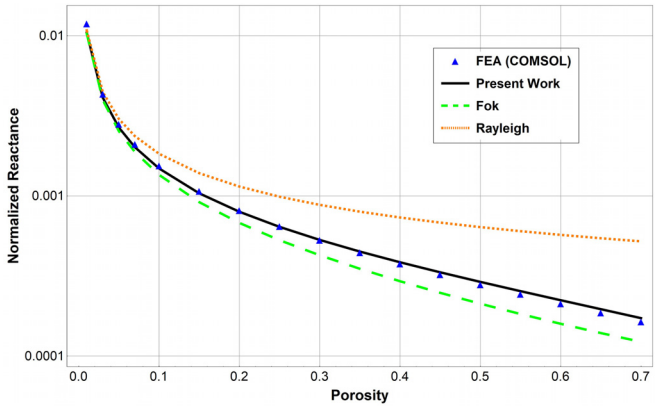

Fig. 3. (Color online) Comparison of the perforated-plate reactance models.

by curve fitting to the numerical results for $1 < \lambda < 14$, where λ is defined following Eq. (1). They calculated the resistive end corrections to be mainly a function of the shear wave-number as

$$\alpha = -\left(0.12/\lambda^3\right) + \left(2.3/\lambda^2\right) + \left(2.76/\lambda\right) + 1.48. \tag{12}$$

There seems to be a lack of general agreement on the resistive end correction. Here, using the same approach used for the reactive part, but now for the real part of the impedance, we use the FEM results to calculate the resistive end length correction. The resistive length correction was determined by curve fitting and using a least square method ($R^2 = 0.96$). The resistive length correction was found to be dependent on the radius of the hole only and the effect of other parameters was negligible

$$l_{er} = 0.94r. \tag{13}$$

We find the resistive end correction to be independent of the porosity. Hence the interaction effects are found to be negligible for the resistive part of the impedance.

In Fig. 4(a), different models for the resistive part of the impedance with different end corrections are compared with the results of COMSOL FEM simulations and with the proposed model for a perforated plate with 3 μm thickness and 16 μm pitch at 1000 Hz. Since the solutions of Ingard (1953), Guo *et al.* (2008), and Bolton and Kim (2010) give very similar results for this case, they are represented with only one curve. Similar to the reactive part, all models are in a good agreement at low porosities. The models deviate from each other as the porosity increases. The result given by the proposed formula is in a good agreement with the numerical results in the whole range of porosities.

In order to understand the dissipation mechanism, the power dissipation density (with the unit of W/m^3) in the FEM domain for two adjacent cells is shown in Fig. 4(b). Most of the interior losses occur along the walls of the holes. The losses

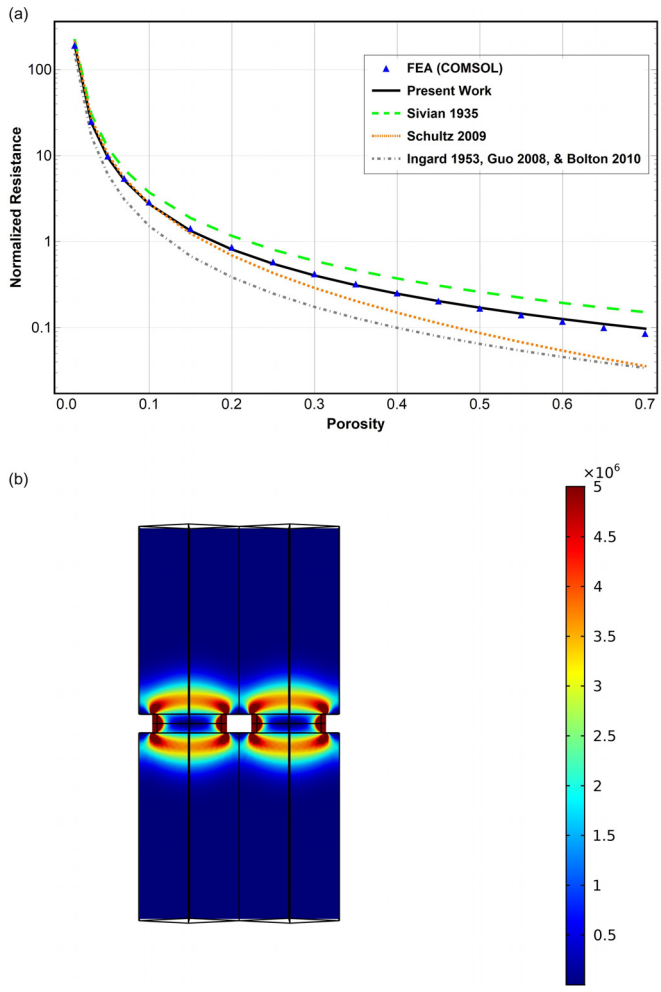

Fig. 4. (Color online) (a) Comparison of the perforated-plate resistance models. (b) Power dissipation density.

corresponding to the end effects occur in the caps within the flow immediately on top and bottom of the holes [noted in Herdtle *et al.* (2013) also] not on the planar surfaces on each side of the holes. This is in contradiction with the assumptions made in the literature over the past few decades, that assume the resistive end effects are due to the friction losses at the planar surfaces on sides of the plates.

3. Conclusions

In this work, the acoustic end effects in micro-perforated plates are studied. Numerical results of thermoviscous acoustic FEM are combined with the analytical solution for cylindrical tubes to calculate the resistive and reactive end effect corrections. The reactive end correction is found to depend on hole radius and porosity. The interaction effect function is found to be a simple function of the porosity, different from previously proposed functions. The resistive end length correction is also calculated and found to be a function of the hole radius only. The resistive end correction is found to be approximately half of the reactive end correction at low porosities. Utilizing FEM, it is shown that the resistive end effects are mostly due to the losses in the area immediately on the top and bottom of the holes and not the friction on the planar surfaces. This is in contradiction with the common hypotheses in the literature. The analytical solution with the proposed end effect corrections matches the FEM results over a wide range of porosities. The proposed model can be used in modeling and optimization studies of MPP and MEMS.

References and links

Bolton, J. S., and Kim, N. (**2010**). "Use of CFD to calculate the dynamic resistive end correction for micro-perforated materials," Acoust. Aust. **38**(3), 134–139.

Guo, Y., Allam, S., and Abom, M. (**2008**). "Micro-perforated plates for vehicle applications," in *37th International Congress and Exhibition on Noise Control Engineering*, Shanghai, China, October.

Herdtle, T., Stuart Bolton, J., Kim, N. N., Alexander, J. H., and Gerdes, R. W. (**2013**). "Transfer impedance of microperforated materials with tapered holes," J. Acoust. Soc. Am. **134**(6), 4752–4762.

Ingard, U. (**1953**). "On the theory and design of acoustic resonators," J. Acoust. Soc. Am. **25**(6), 1037–1061.

Kampinga, W. R. (**2010**). "Viscothermal acoustics using finite elements—Analysis tools for engineers," Ph.D. thesis, University of Twente, Netherlands.

Kuntzman, M. L., LoPresti, J. L., Du, Y., Conklin, W. F., Naderyan, V., Lee, S. B., Schafer, D., Pedersen, M., and Loeppert, P. V. (**2018**). "Thermal boundary layer limitations on the performance of micromachined microphones," J. Acoust. Soc. Am. **144**(5), 2838–2846.

Maa, D. Y. (**1998**). "Potential of microperforated panel absorber," J. Acoust. Soc. Am. **104**(5), 2861–2866.

Mechel, F. P., and Munjal, M. L. (**2008**). *Formulas of Acoustics* (Springer, Berlin).

Melling, T. H. (**1973**). "The acoustic impedance of perforates at medium and high sound pressure levels," J. Sound Vib. **29**(1), 1–65.

Pierce, A. D. (**1981**). *Acoustics; an Introduction to its Physical Principles and Applications* (Acoustical Society of America and American Institute of Physics, New York).

Rayleigh, L. (**1877**). *The Theory of Sound*, 2nd ed. (Dover, New York), Vol. 2.

Schultz, T., Liu, F., Cattafesta, L., Sheplak, M., and Jones, M. (**2009**). "Comparison study of normal-incident acoustic impedance measurements of a perforate liner," in *15th AIAA/CEAS Aeroacoustics Conference (30th AIAA Aeroacoustics Conference)*, p. 3301.

Sivian, L. J. (**1935**). "Acoustic impedance of small orifices," J. Acoust. Soc. Am. **7**(2), 94–101.

Temiz, M. A., Arteaga, I. L., Efraimsson, G., Abom, M., and Hirschberg, A. (**2014**). "Acoustic end correction in micro-perforated plates-revisited," in *Proceedings of ICSV-21*, pp. 1–7.

Tijdeman, H. (**1975**). "On the propagation of sound waves in cylindrical tubes," J. Sound Vib. **39**(1), 1–33.

Younis, M. (**2011**). *MEMS Linear and Nonlinear Statics and Dynamics* (Springer, New York).